Received: 3 February 2022 | Revised: 15 September 2022 | Accepted: 21 October 2022

DOI: 10.4218/etrij.2022-0001

ORIGINAL ARTICLE

ETRI Journal WILEY

Direct tracking of noncircular sources for multiple arrays via improved unscented particle filter method

Yang Qian[1,2] | Xinlei Shi[1,2] | Haowei Zeng[1,2] | Mushtaq Ahmad[1,2]

[1]College of Electronic Information Engineering, Nanjing University of Aeronautics and Astronautics, Nanjing, China

[2]Key Laboratory of Dynamic Cognitive System of Electromagnetic Spectrum Space (Nanjing University of Aeronautics and Astronautics), Ministry of Industry and Information Technology, Nanjing, China

Correspondence
Yang Qian, College of Electronic Information Engineering, Nanjing University of Aeronautics and Astronautics. Nanjing, China.
Email: qianyang@nuaa.edu.cn

Abstract

Direct tracking problem of moving noncircular sources for multiple arrays is investigated in this study. Here, we propose an improved unscented particle filter (I-UPF) direct tracking method, which combines system proportional symmetry unscented particle filter and Markov Chain Monte Carlo (MCMC) algorithm. Noncircular sources can extend the dimension of sources matrix, and the direct tracking accuracy is improved. This method uses multiple arrays to receive sources. Firstly, set up a direct tracking model through consecutive time and Doppler information. Subsequently, based on the improved unscented particle filter algorithm, the proposed tracking model is to improve the direct tracking accuracy and reduce computational complexity. Simulation results show that the proposed improved unscented particle filter algorithm for noncircular sources has enhanced tracking accuracy than Markov Chain Monte Carlo unscented particle filter algorithm, Markov Chain Monte Carlo extended Kalman particle filter, and two-step tracking method.

KEYWORDS

direct tracking, improved unscented particle filter method, multiple arrays, noncircular sources

1 | INTRODUCTION

Wireless location technology is an important research direction, while wireless positioning technology is widely used in aviation, indoor positioning, navigation, geological exploration, and other fields [1]. The two-step localization method obtains the target position through time, angle, frequency difference, and other parameters [2]. In addition, it also brings significant estimation errors because it has gone through many estimation steps [3]. Direct positioning technology can use complete information, and positioning accuracy is more accurate [4]. Standard direct location algorithms include subspace data fusion, capon, and propagator [5].

The traditional direct location is aimed at where the source remains unchanged. Now, we begin to study moving sources with multiple stations. Passive emitter state estimation by time delay and Doppler frequency shift is widely used in radar, sonar, satellite positioning, and navigation. In real time, the receiving station uses its position and received emitter signal to calculate the target position, velocity, and other state parameters [6]. The traditional two-step tracking algorithm first estimates the intermediate parameters and then solves the observation equation composed of the intermediate parameters to obtain the target tracking trajectory, such as arrival angle, arrival time difference, and arrival frequency difference [7]. It is a typical application of the intermediate parameter estimation method in the two-step method, but in the parameter estimation stage, the two-step method ignores the connection between observation stations and loses some position information, and the introduced errors are superimposed and accumulated continuously [8]. Therefore, the two-step tracking algorithm is suboptimal.

In contrast, the direct tracking algorithm proposed in recent years does not require parameter estimation and location [9]. Unlike the two-step tracking method, direct tracking does not need to estimate the time-frequency difference parameters of the target signal but directly establishes the observation equation based on the received signal. The solution is calculated step-by-step but directly estimates the target position based on the sampled signal, which avoids the shortcomings of the two-step tracking algorithm and can obtain a better positioning effect, which has been widely studied.

The direct tracking problem of noncircular sources is introduced. The noncircular source is one of the most studied signals [10, 11]. Noncircular sources are the same phase component in amplitude with zero orthogonal components. BPSK, ASK, AM, and PAM modulated sources are common in modern communication and satellite systems. Therefore, the study of noncircular sources has important practical significance for direct location algorithms [12–14].

The particle filter has a good effect and a wide application range, while the Kalman filter has a small amount of calculation and is less time-consuming. Combining the two filtering algorithms, the extended Kalman Particle filter (EPF) and unscented particle filter (UPF) appear, respectively. Firstly, extended Kalman filter and unscented Kalman filter are used as the recommended distribution function and then the PF method is used for processing [15–18]. However, the filtering accuracy of UPF sometimes cannot meet the requirements of high-precision and high-dynamic target tracking. The basic idea of the Markov Chain Monte Carlo method establishes a Markov chain with the goal of stable distribution by defining state space variables and using the Markov chain to obtain the samples of function. We combine the Markov Chain Monte Carlo method and the system proportional symmetry method with UPF to form the system proportional symmetry Markov Chain Monte Carlo particle filter algorithm [19–27].

The contributions of this paper are as follows:

- We propose a direct tracking method to use multiple observation stations to estimate the moving target position directly, which avoids the shortcomings of the two-step localization algorithm and can obtain a better localization effect.
- We introduce noncircular sources into the direct tracking scene. The performance of the particle filter algorithm under the noncircular sources is better than that under the circular sources.
- We propose an improved UPF (I-UPF) direct tracking method that combines system proportional symmetry UPF and Markov Chain Monte Carlo algorithm to improve the positioning accuracy in direct tracking.

The structure of this paper is organized as follows. In Section 2, we introduce the system model of the direct tracking method. Section 3 describes the I-UPF direct tracking algorithm. Section 4 analyzes the performance analysis of I-UPF and other direct tracking algorithms. In the next section, we emulate the I-UPF algorithm for noncircular sources with multiple uniform arrays and make a corresponding comparison under different iterations and particles. Furthermore, we summarize this paper in Section 5.

The following notations are as follows: $(\cdot)^{\mathrm{T}}$ denotes transposition, $(\cdot)^{\mathrm{H}}$ denotes conjugate transpose, and $(\cdot)$ *denotes the conjugate. The symbol $\|\cdot\|$ denotes the Euclidean norm.

2 | SYSTEM MODEL

In this section, we introduce a few notions about the model of direct tracking, then we introduce the noncircular sources model and characteristics.

Suppose there is a uniform, straight line in each observation station in two-dimensional space. The moving target radiates three noncircular radio sources with bandwidth W and carrier frequency f_c. Assuming that the target of the observation station is in a fixed state, the number of observation stations is L; each observation station is placed with a linear array of eight uniform array elements, and the motion state of each target at the kth snapshot time is expressed as $\mathbf{d}_k=\left[d_x,\dot{d}_x,d_y,\dot{d}_y\right]^{\mathrm{T}}$, which $\overline{\mathbf{d}}_k=\left[d_x,d_y\right]^{\mathrm{T}}$ represents the target position component and $\dot{\mathbf{d}}_k=\left[\dot{d}_x,\dot{d}_y\right]^{\mathrm{T}}$ represents the target velocity component. The scene diagram of direct tracking is displayed as shown in Figure 1.

Suppose there are L fixed receiving stations in space, Q sources, and targets, and eight array elements are arranged on each observation station, which is synchronous in time and frequency. The receiving station intercepts the radiation source signal within K observation intervals. It indicates the position coordinates of the receiving station in the kth ($k=1, 2, 3, \ldots, K$) sampling snapshot time and the number of sampling points v_k.

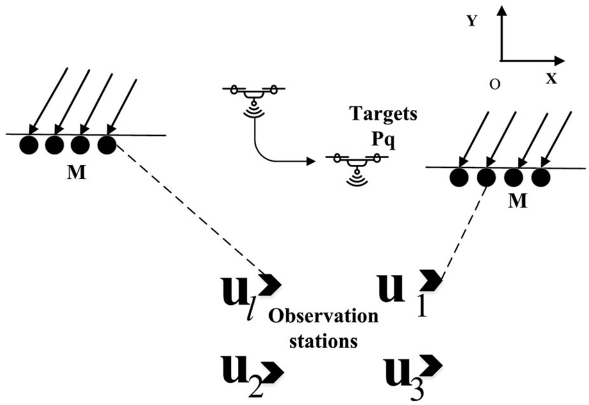

FIGURE 1 The scene diagram of direct tracking.

Set as the signal sent by the target, assuming that the signal model is

$$s(t) = x(t)e^{j2\pi f_c t}, \tag{1}$$

where f_c is the carrier frequency and $x(t)$ is the envelope of sources. If the number of sampling points is v_k, the signal received by the receiving station at the kth snapshot time of lth receiving station is [2].

$$\mathbf{z}_{l,k}(v_k) = \mathbf{A}_l(\mathbf{p})\mathbf{s}_{l,q}\left(v_k - \frac{\tau_{l,q}}{T_s}\right) + \mathbf{n}_l(v_k),\ v_k = 1, 2, ..., V_k, \tag{2}$$

$$\mathbf{A}_l(\mathbf{p}) = [\mathbf{a}_l(\mathbf{p}_1), ..., \mathbf{a}_l(\mathbf{p}_Q)], \tag{3}$$

$$\mathbf{a}_l\left(\mathbf{p}_q\right) = \left[1\ e^{j2\pi d f_{l,q} \mathrm{T}_s v_k}\ ...\ e^{j2\pi(M-1)d f_{l,q}\mathrm{T}_s v_k}\right]^{\mathrm{T}}, \tag{4}$$

where j represents the imaginary part, T_s is the sampling period, $s_{l,k}(t)$ is the signal of the kth observation interval target of the lth observation station, $n_{l,k}(t)$ is the generalized stationary complex Gaussian white noise with zero mean, its covariance matrix is $\mathbf{\Gamma}_{l,k} = \sigma_n 2\mathbf{I}$, $\tau_{l,k}$ is the time delay of the signal reaching the lth receiving station, and $f_{l,k}$ is the Doppler frequency shift caused by the relative displacement between the lth receiving station and the target, respectively:

$$\tau_{l,k} = \frac{\left\|\mathbf{u}_{l,k} - \overline{\mathbf{d}}_k\right\|}{c}, \tag{5}$$

$$f_{l,k} = \frac{f_c}{c}\frac{\left(\mathbf{u}_{l,k} - \overline{\mathbf{d}}_k\right)^{\mathrm{T}}\mathbf{d}_k}{\left\|\mathbf{u}_{l,k} - \overline{\mathbf{d}}_k\right\|}, \tag{6}$$

where c is the propagation speed of the signal and $\|\cdot\|$ represents the Euclidean norm. It is proposed in the literature [27] that s_k $(v_k - \tau_{l,k}/T_s)$ uses the discrete Fourier transform and inverse transform to avoid introducing quantization error through the time delay information of the signal. Suppose that after the Fourier transform and inverse transform of time delay information,

$$\mathbf{z}_{l,k} = \mathbf{A}_{f_{l,k}}\mathbf{G}^{\mathrm{H}}\mathbf{A}_{\tau_{l,k}}\mathrm{G}s_k\mathbf{A}_l(\mathbf{p}) + \mathbf{n}_{l,k} = \mathbf{H}_{l,k}\mathbf{s}_k\mathbf{A}_l(\mathbf{p}) + \mathbf{n}_{l,k}, \tag{7}$$

where $\mathbf{G}$ represents the discrete DFT matrix, $\mathbf{G}^{\mathrm{H}}$ represents the conjugate transpose of the matrix $\mathbf{G}$, $\mathbf{A}_{f_{l,k}}$ is the Doppler frequency shift matrix, $\mathbf{A}_{\tau_{l,k}}$ is the time delay matrix, and its expressions are as follows:

$$G = \frac{1}{V_k}\exp\left(\frac{-j2\pi v_k v_k^{\mathrm{T}}}{V_k}\right), \tag{8}$$

$$\mathbf{A}_{f_{l,k}} = \mathrm{diag}\{\exp(j2\pi T_s f_{l,k} v_k)\}, \tag{9}$$

$$\mathbf{A}_{\tau_{l,k}} = diag\left\{\exp\left\{\frac{-j2\pi}{\frac{V_k v_k \tau_{l,k}}{T_s}}\right\}\right\}, \tag{10}$$

$$\mathbf{H}_{l,k} = \mathbf{A}_{f_{l,k}}\mathbf{G}^{\mathrm{H}}\mathbf{A}_{\tau_{l,k}}\mathbf{G}. \tag{11}$$

Then the received signal observation equation of all observation stations is expressed as follows:

$$\mathbf{z}_k = \mathbf{H}_k\mathbf{s}_k\mathbf{A}_l(\mathbf{p}) + \mathbf{n}_k, \tag{12}$$

where

$$\begin{cases} \mathbf{z}_k = \left[\mathbf{z}_{1,k}^{\mathrm{T}}\ \mathbf{z}_{2,k}^{\mathrm{T}}\ ...\ \mathbf{z}_{L,k}^{\mathrm{T}}\right]^{\mathrm{T}}, \\ \mathbf{n}_k = \left[\mathbf{n}_{1,k}^{\mathrm{T}}\ \mathbf{n}_{2,k}^{\mathrm{T}}\ ...\ \mathbf{n}_{L,k}^{\mathrm{T}}\right]^{\mathrm{T}}, \\ \mathbf{H}_k = \left[\mathbf{H}_{1,k}^{\mathrm{T}}\ \mathbf{H}_{2,k}^{\mathrm{T}}\ ...\ \mathbf{H}_{L,k}^{\mathrm{T}}\right]^{\mathrm{T}}. \end{cases} \tag{13}$$

When the transmission signal and path propagation attenuation coefficient are unknown, the receiving station directly intercepts the radio signal radiated by the moving target. It establishes the observation equation about the target state. This paper aims to accurately estimate the X-axis, Y-axis, and target velocity of the moving target through the known nonlinear observation information.

For noncircular sources, the covariance matrix and elliptic covariance matrix satisfy

$$\mathrm{E}\left[\mathbf{s}_l(k)\mathbf{s}_l^{\mathrm{H}}(k)\right] = \rho e^{j\varphi}\mathrm{E}\left[\mathbf{s}_l(k)\mathbf{s}_l^{\mathrm{T}}(k)\right], \tag{14}$$

where φ is the noncircular phase and ρ is the noncircular rate of the value in $0 \sim 1$.

The noncircular sources rate of 1 is the leading noncircular rate source. This paper supposes that the rate of noncircular sources is 1.

According to Dai and others [10], noncircular sources can be expressed as follows:

$$\mathbf{s}_l(k) = [s_{l,1}(k) \;\; s_{l,2}(k) \;\; \dots \;\; s_{l,Q}(k)]^{\mathrm{T}}. \tag{15}$$

The noncircular sources at the kth snapshot time of the lth observation station can be expressed as follows:

$$s_{l,i}(k) = s_{l,i}^{(0)}(k) e^{j\varphi_i}, \tag{16}$$

$$s_l(k) = \begin{bmatrix} s_{l,1}(k) \\ s_{l,2}(k) \\ \vdots \\ s_{l,Q}(k) \end{bmatrix} = \begin{bmatrix} s_{l,1}^{(0)} e^{j\varphi_1} \\ s_{l,2}^{(2)} e^{j\varphi_2} \\ \vdots \\ s_{l,Q}(k) e^{j\varphi_Q} \end{bmatrix} = \mathbf{\Phi} \begin{bmatrix} s_{l,1}^{(0)} \\ s_{l,2}^{(2)} \\ \vdots \\ s_{l,Q}(k) \end{bmatrix}, \tag{17}$$

$$\mathbf{\Phi} = \begin{bmatrix} e^{-j\varphi_1} & 0 & \dots & 0 \\ 0 & e^{-j\varphi_2} & \ddots & \vdots \\ \vdots & \vdots & \ddots & 0 \\ 0 & \dots & 0 & e^{-j\varphi_Q} \end{bmatrix}, \tag{18}$$

$$\mathbf{s}_l^0(k) = \left[\mathbf{s}_{l,1}^{(0)}(k),\, \mathbf{s}_{l,2}^{(0)}(k),\, \dots,\, \mathbf{s}_{l,Q}^{(0)}(k)\right]^{\mathrm{T}}. \tag{19}$$

Taking advantage of the fact that the elliptic covariance matrix of a noncircular signal is not zero, the received signal vector of the lth observation station can be extended to

$$\mathbf{r}_l(k) = \begin{bmatrix} \mathbf{z}_l(k) \\ \mathbf{z}_l^*(k) \end{bmatrix} = \begin{bmatrix} \mathbf{A}_l(\mathbf{p}) \\ \mathbf{A}_l(\mathbf{p})\mathbf{\Phi}^*\mathbf{\Phi}^* \end{bmatrix} \mathbf{H}_l(k)\mathbf{s}_l(k) + \begin{bmatrix} \mathbf{n}_l(k) \\ \mathbf{n}_l^*(k) \end{bmatrix}. \tag{20}$$

Simultaneous all observation equations

$$\mathbf{r}_k = \left[\mathbf{r}_{1,k}^{\mathrm{T}} \;\; \mathbf{r}_{2,k}^{\mathrm{T}} \;\; \dots \;\; \mathbf{r}_{L,k}^{\mathrm{T}}\right]^{\mathrm{T}}. \tag{21}$$

3 | THE PROPOSED I-UPF METHOD

UPF algorithm essentially uses UKF filtering to obtain a proposed distribution function and then uses this proposed distribution function to replace the importance density function $p(\mathbf{d}_k^i|\mathbf{d}_{k-1}^i, \mathbf{r}_k)$ in the classical PF algorithm. In the high-precision and dynamic direct tracking problem, the accuracy of the UPF algorithm needs to be improved. SPSUPF algorithm makes two improvements based on UPF: first, the selection of Sigma sampling points is adjusted appropriately to improve the accuracy of UT transform. The second is to improve the resampling algorithm in the later PF, adopt the system resampling method, effectively solve the problem of particle degradation, and set the threshold in the resampling process, so it is not necessary to resample all sample points and reduce the amount of calculation.

3.1 | SPSUPF algorithm for direct tracking

UPF has similar advantages to UKF. For example, it does not need to calculate the Jacobian matrix of nonlinear system measurement and state equations. However, the estimation accuracy of the system state can reach at least second order, which is easier to implement than EPF, and the accuracy is higher. Furthermore, the UPF algorithm uses UKF filtering to obtain a proposed distribution function and then uses this proposed distribution function to replace the importance density function in the classical PF algorithm.

After a set of observations is given, let the total number of particles be H, the total number of iterations be K, the ith sampling particle in the kth iteration, and the particle weight be ψ_k^i. Initial sampling $\mathbf{d}_k^i$ is conducted, and particles are extracted from the known initial distribution to generate a set of sample points that obey the $p(\mathbf{d}_0)$ distribution. In the kth iteration, the posterior probability density function can be expressed as follows:

$$p(\mathbf{d}_k|\mathbf{r}_k) \approx \sum_{i=1}^{V} \psi_k^i \delta\left(\mathbf{d}_k - \mathbf{d}_k^i\right). \tag{22}$$

According to the theorem of large numbers, it will converge to the real a posteriori probability when it is large enough. The particle weight calculation formula is

$$\psi_k^i = \psi_{k-1}^i \frac{p\left(\mathbf{r}_k|\mathbf{d}_k^i\right) p\left(\mathbf{d}_k^i|\mathbf{d}_{k-1}^i\right)}{q\left(\mathbf{d}_k^i|\mathbf{d}_{k-1}^i, \mathbf{r}_k\right)}. \tag{23}$$

The filter estimation and variance are calculated, and the UKF algorithm obtains the filter estimation and the particle set. The recommended distribution density function is as follows:

$$q(\mathbf{d}_k|\mathbf{d}_{k-1}, \mathbf{r}_k) = N\left(\hat{\mathbf{d}}_k, \mathbf{P}_k^i\right). \tag{24}$$

In the process of generating the proposed distribution function by SPSUPF, the proportional symmetric sampling algorithm is adopted, and the selection of weight coefficients is changed. The first-order and second-order weight coefficients corresponding to the UT transform [19, 20] are as follows:

$$\begin{cases} R_i^m = \begin{cases} \gamma/(n+\gamma)(i=0), \\ 1/2(n+\gamma)(i \neq 0), \end{cases} \\ R_i^c = \begin{cases} \gamma/(n+\gamma)+1+\varepsilon-\beta^2(i=0), \\ 1/2(n+\gamma)(i \neq 0), \end{cases} \end{cases} \tag{25}$$

where $\gamma = \beta^2(n+k) - n$ is the scale parameter, n represents the dimension of the system state, and k is a scale parameter. In general, the semipositive nature of a posteriori covariance should be ensured. For the case of Gaussian distribution, when the state variable is univariate, $k \neq 0$. When the status variable is multidimensional, it is generally selected $k = 0$. β is the scaling factor. The distance from the Sigma point to the center point can be adjusted by adjusting the value. Therefore, proportional symmetric sampling can effectively solve the problem that the distance from the sigma point to the center point becomes farther and farther with the increased dimension of the system state vector, resulting in the nonlocal effect of sampling. ε represents the prior distribution information of the state vector and improves the covariance's approximation accuracy by combining the higher-order terms' dynamic differences in the covariance.

Weight normalization processing

$$\psi_k^i = \frac{\psi_k^i}{\sum_{i=1}^{N} \psi_k^i}. \tag{26}$$

For general resampling methods, a resampling threshold needs to be set. When the adequate particle capacity is less than the threshold, degradation will occur. Therefore, resampling is introduced based on the original importance sampling to eliminate the particles with low weight and concentrate the particles with high weight. To better suppress the degradation phenomenon, the system resampling algorithm is introduced into SYSUPF. The time complexity of system resampling is equivalent to that of ordinary resampling, and the filtering accuracy can be improved under the same conditions.

Use the system resampling algorithm. Set the adequate particle capacity $N_{\text{eff}} = 1/\sum_{i=1}^{N} \left(\psi_k^i\right)^2 N_{\text{th}} = N/3$ if it means that the system samples are seriously degraded. It is necessary to resample $\left\{\mathbf{d}_k^i \ \ \psi_k^i\right\}$, $i = 1, 2, ..., N$ to obtain a new particle set $\left\{\widehat{\mathbf{d}}_k^i \ \ \widehat{\psi}_k^i\right\}$, $\widehat{\psi}_k^i = 1/N$, $i = 1, 2, ..., N$, and the result is output

$$\mathbf{d}_k^i = \sum_{i=1}^{N} \widehat{\psi}_k^i \widehat{\mathbf{d}}_k^i, \tag{27}$$

$$\mathbf{P}_k = \sum_{i=1}^{N} \widehat{\psi}_k^i \left(\widehat{d}_k^i - d_k\right) \left(\widehat{d}_k^i - d_k\right)^{\mathrm{T}}. \tag{28}$$

3.2 | MCMC algorithm

The MCMC algorithm is used to estimate the posterior probability distribution of the target in the sequential iteration of the particle filter to steer clear of the problem of particle dilution. The core idea of the MCMC algorithm is to obtain approximately obeying $p(\mathbf{d}_k|\mathbf{r}_k)$ random samples by establishing a Markov chain with stable distribution $p(\mathbf{d}_k|\mathbf{r}_k)$ and then use these samples for various statistics. The Markov chain composed of the MCMC algorithm has good convergence [23]. Since the observation model of direct tracking is highly nonlinear, its likelihood function can be approximately expressed as follows:

$$p(\mathbf{r}_k|\mathbf{d}_k) \propto \exp\left\{ -\frac{1}{\sigma_n^2} \sum_{l=1}^{L} \|\mathbf{r}_{l,k} - \mathbf{A}_l(\mathbf{p})\mathbf{H}_{l,k}\mathbf{s}_k\|^2. \right. \tag{29}$$

The expression of the generalized likelihood function derived from the maximum a posteriori estimation criterion is [23].

$$p(\mathbf{r}_k|\mathbf{d}_k) \propto \exp\left\{ \frac{1}{\sigma_n^2} \lambda_{\max}(\mathbf{\Phi}_k) \right\}, \tag{30}$$

where $\mathbf{\Phi}_k$ is the matrix of $L \times L$, and its expression is as follows:

$$\mathbf{\Phi}_k = (\mathbf{U}_k)^{\mathrm{H}} \mathbf{U}_k, \tag{31}$$

$$\mathbf{U}_k = \left[(\mathbf{H}_{1,k})^{\mathrm{H}} \mathbf{r}_{1,k}, \ ..., \ (\mathbf{H}_{L,k})^{\mathrm{H}} \mathbf{r}_{L,k} \right]. \tag{32}$$

3.3 | The procedure of the proposed algorithm

We summarize several steps about I-UPF algorithms as follows. Furthermore, Figure 2 describes the algorithm flow chart.

Step 1. Establish a time-frequency equation of direct tracking and adopt noncircular sources.

Step 2. Initialization. The prior probability distribution $p(\mathbf{d}_0)$ is sampled to obtain the particle set with the number of particles $\left\{\mathbf{d}_0^1, \mathbf{d}_0^2, ..., \mathbf{d}_0^N\right\}$, and all sample weights ψ_k^j are set $1/N$.

Step 3. Calculate the filter estimate and variance. The UKF algorithm obtains the filter estimation and variance of the particle set. The proportional symmetric sampling algorithm is used to select Sigma points, improving UT transform accuracy.

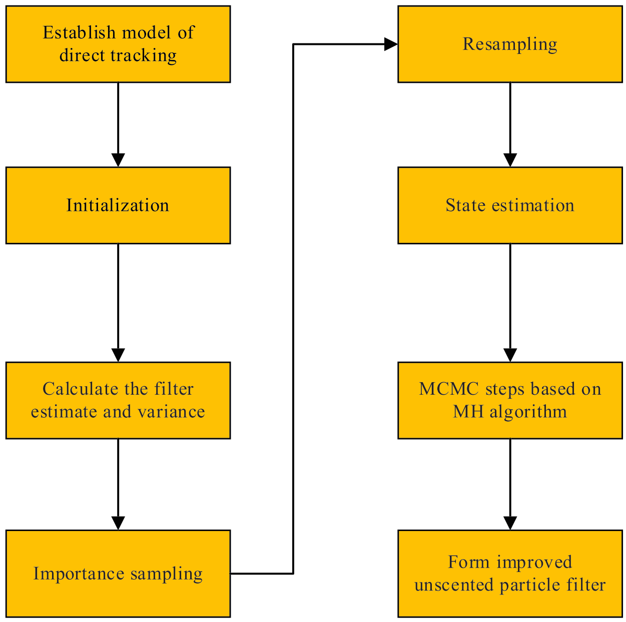

FIGURE 2 Algorithm flow chart.

Step 4. Importance sampling, sampling from $\mathbf{d}_k^i \to q\left(\mathbf{d}_k^i | \mathbf{d}_{k-1}^i, \mathbf{r}_k\right) = N\left(\widehat{\mathbf{d}}_k^i, \widehat{\mathbf{P}}_k^i\right)$, updating particles.

Step 5. Importance weight calculation. The importance weight of particles is calculated and normalized.

Step 6. Resampling. Calculate N_{eff}, if necessary, resample to obtain a new particle set $\left\{\widehat{\mathbf{d}}_k^i \ \widehat{\psi}_k^i\right\}$, $\widehat{\psi}_k^i = 1/N$, $i = 1, 2, ..., N$.

Step 7. State estimation $\widehat{\mathbf{d}}_k = \sum_{i=1}^{N} \psi_k^i \mathbf{d}_k^{i*}$.

Step 8. MCMC steps are based on the MH algorithm.

Step 9. Form improved the I-UPF direct tracking method, combining system proportional symmetry UPF and Markov Chain Monte Carlo algorithm.

4 | PERFORMANCE ANALYSIS

In this chapter, the computational complexity, the I-UPF algorithm's performance of the I-UPF algorithm, and the spatial degree of freedom (DOF) are analyzed, and we describe the preponderances of the I-UPF algorithm.

4.1 | Achievable DOFs

We define that M denotes the array element number. The noncircular sources increase the number of received sources. Therefore, the DOF of the proposed algorithm for noncircular sources increases to $2M$ as shown in Table 1.

TABLE 1 DOF of different sources.

Different sources	DOF
Circular sources	M
Noncircular sources	2M

TABLE 2 Calculation time of different algorithm.

Algorithms	Time (s)
I-UPF	18.3863
UPF-MCMC	20.0362
EPF–MCMC	17.8441
PF-MCMC	13.6161
PF-TDOA	22.0924
PF	11.5436

Abbreviations: EPF, Extended Kalman particle filter; I-UPF, improved unscented particle filter; PF, particle filter.

4.2 | Complexity analysis

It can be observed that the calculation time shows that the improved particle filter algorithm has lower computational complexity. N represents the number of particles, M represents array numbers, L represents the number of observation stations, and K denotes snapshot numbers. The complexity of the I-UPF algorithm contains several aspects: the calculation of the initialization part $O(NML)$, the calculation of particle weight $O(M^2KL + NL)$, and the calculation of state estimation $O(4M^3LK + ML)$. The total complexity is $O(NML + M^2KL + NL + 4M^3LK + ML)$. From Table 2, the I-UPF algorithm has slightly higher computational complexity than the EPF–MCMC and PF-MCMC algorithms. The I-UPF algorithm has lower computational complexity than UPF-MCMC and two-step tracking algorithms, but the direct tracking performance is greatly improved. The simulation in the next chapter will express this in detail.

4.3 | Advantages

We analyze the preponderances of the proposed algorithm with noncircular sources for direct tracking.

- We adopt a direct tracking method to estimate the target position based on the sampled signal, which avoids the shortcomings of the two-step localization algorithm.
- Noncircular sources for direct tracking can extend the dimension of the received source matrix and improve positioning accuracy.

- We propose an improved UPF direct tracking method that combines system proportional symmetry UPF and Markov Chain Monte Carlo algorithm to improve the positioning accuracy in direct tracking.

5 | SIMULATION RESULTS

In this chapter, we emulate the I-UPF algorithm for noncircular sources, obtain the direct tracking diagram, and compare the performance of the I-UPF algorithm with other direct tracking algorithms. As shown in the following Figure 3, the multitarget tracking scene is displayed. There are four observation stations and three targets. Each station has a linear array of eight uniform array elements. Observation stations are $u_1=[-600\text{ m}\quad 100\text{ m}]$, $u_2=[-700\text{ m}\quad 1000\text{ m}]$, $u_3=[1500\text{ m}\quad 1100\text{ m}]$, $u_4=[1400\text{ m}\quad 120\text{ m}]$. The starting speed is $\mathbf{d}=[100\text{ m/s}\quad 100\text{ m/s}]^{\mathrm{T}}$. The target moves in a straight line and two curve lines at a uniform speed.

The tracking estimation performance is analyzed by calculating the root-mean-square error (RMSE), RMSE of target position, and RMSE of speed, and it can be denoted as

$$\mathbf{r}_{\mathrm{RMSE}}(k)=\sqrt{\mathrm{E}\left\{\left\|\overline{\mathbf{d}}_k-\widehat{\mathbf{d}}_k\right\|^2\right\}}, \tag{33}$$

$$\mathbf{r}_{\mathrm{RMSE}}(k)=\sqrt{\mathrm{E}\left\{\left\|\dot{\mathbf{d}}_k-\widetilde{\mathbf{d}}_k\right\|^2\right\}}, \tag{34}$$

where $\widehat{\mathbf{d}}_k$ is at kth snapshot time position estimation and $\widetilde{\mathbf{d}}_k$ is at kth snapshot time speed estimation. Set signal-to-noise ratios (SNR) = 10 dB, Monte Carlo 500 times, number of particles $N_p=200$, and the total length of Markov chain is 500, where the number of iterations is set $N=150$.

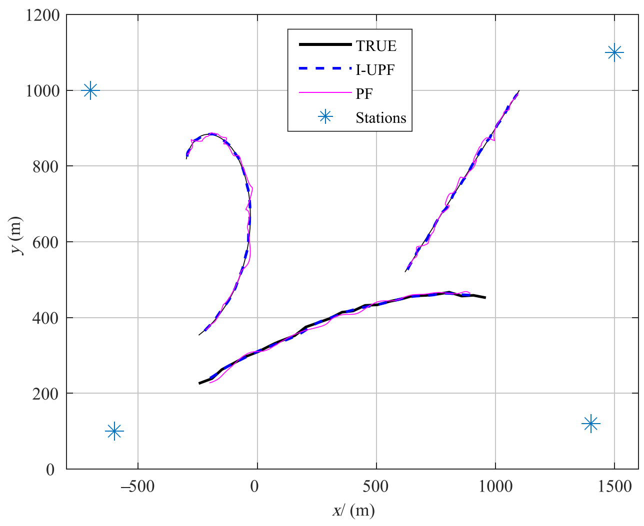

FIGURE 3 Multitarget tracking scene.

Three moving targets and four observation stations are in the set scene. Three moving targets and four observation stations are in the set scene. Four observation stations are $u_1=[-600\text{ m}\quad 100\text{ m}]$, $u_2=[-700\text{ m}\quad 1000\text{ m}]$, $u_3=[1500\text{ m}\quad 1100\text{ m}]$, $u_4=[1400\text{ m}\quad 120\text{ m}]$. Each station has a uniform array. The RMSE results of speed error comparison of the proposed I-UPF algorithm with other algorithms are shown in Figure 4. As the number of iterations increases, the performance of the I-UPF algorithm is better than the EPF–MCMC algorithm, PF-MCMC algorithm, and two-step tracking algorithm.

The RMSE results of error comparison of the proposed I-UPF algorithms with other algorithms under different SNR are shown in Figure 5 below. As SNR increases, the performance of the I-UPF algorithm is

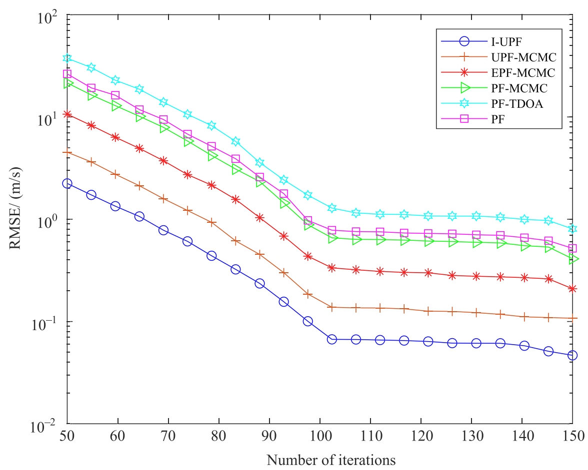

FIGURE 4 The variation of speed tracking error with iterations.

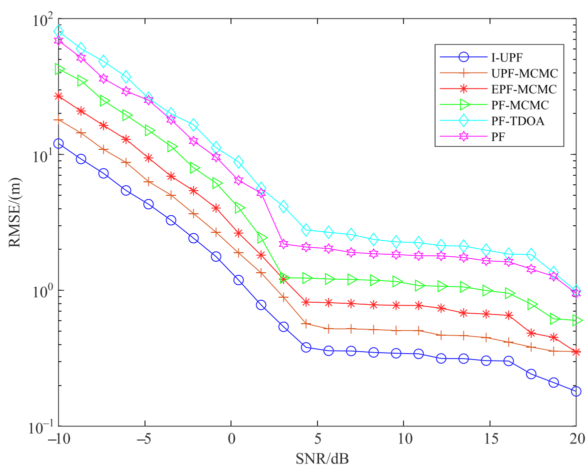

FIGURE 5 The variation of tracking error with signal-to-noise ratio (SNR).

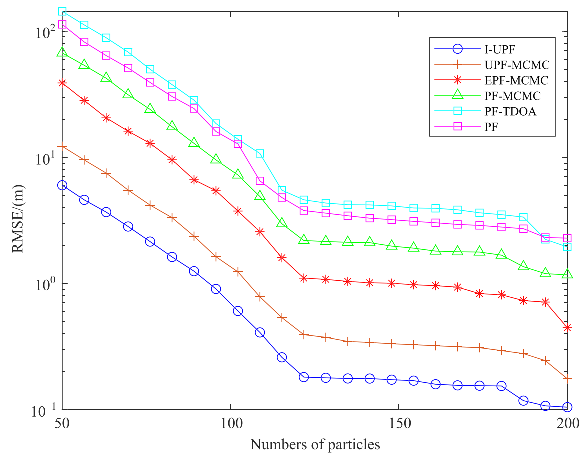

FIGURE 6 Different algorithms with the number of particle filters.

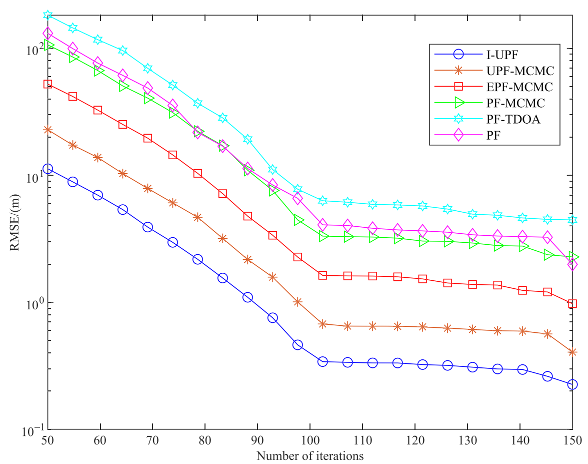

FIGURE 7 Different algorithms with the number of iterations.

better than the EPF–MCMC algorithm, PF-MCMC algorithm, and two-step tracking algorithm.

The RMSE results of the error comparison of the proposed I-UPF algorithms with other algorithms under different particles and iterations are shown in Figures 6 and 7. As the number of particles and iterations increases, the performance of the I-UPF algorithm is better than the EPF–MCMC algorithm, PF-MCMC, PF algorithm, and two-step tracking algorithm. Furthermore, the performance is improved a lot after adding the MCMC algorithm. Figure 8 shows the RMSE results of error comparison about the proposed I-UPF algorithms with other algorithms under circular and noncircular sources. As SNR increases, the performance of the algorithms under noncircular sources is better than that under circular sources. This is because noncircular sources extend the dimension of the sources matrix, and direct tracking accuracy is promoted.

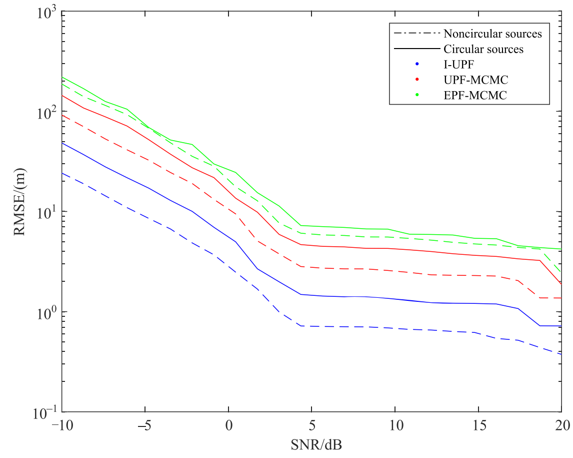

FIGURE 8 Different algorithms with circular sources and noncircular sources.

6 | CONCLUSION

The aim of this study is to promote the accuracy of direct tracking with particle filters. In this study, we propose an I-UPF algorithm, and a uniform array is introduced into the field of direct tracking, combining system proportional symmetry UPF and Markov Chain Monte Carlo algorithm. Noncircular sources extend the dimension of the sources matrix, and direct tracking accuracy is promoted. Simulation results show that the proposed I-UPF algorithm for noncircular sources has improved positioning accuracy than Markov Chain Monte Carlo UPF algorithm, Markov Chain Monte Carlo EPF, and two-step tracking method. Coprime or nested array for direct tracking will improve the degree of freedom and tracking accuracy. Therefore, a sparse array for direct tracking is the focus of future research.

CONFLICT OF INTEREST STATEMENT

The authors declare that there are no conflicts of interest.

ORCID

Yang Qian https://orcid.org/0000-0002-1552-8997
Mushtaq Ahmad https://orcid.org/0000-0003-4280-5766

REFERENCES

1. Y. Wang, Y. Wu, and S. Yi, *An efficient direct position determination algorithm combined with time delay and Doppler*, Circuits Syst. Signal Process. **35** (2016), 635–649. https://doi.org/10.1007/s00034-015-0069-6
2. M. Oispuu and U. Nickel, *Direct detection and position determination of multiple sources with intermittent emission*, IEEE

Trans. Signal Process. **90** (2010), 3056–3064. https://doi.org/10.1016/j.sigpro.2010.05.010
3. J. Yin, D. Wang, and Y. Wu, *An efficient direct position determination method for multiple strictly noncircular sources*, IEEE Sens. J. **18** (2018), no. 2, 324–346. https://doi.org/10.3390/s18020324
4. J. Yin, Y. Wu, and D. Wang, *Direct position determination of multiple noncircular sources with a moving array*, Circuits Syst. Signal Process. **36** (2017), no. 10, 4050–4076. https://doi.org/10.1007/s00034-017-0499-4
5. Y. Zhang, B. Ba, D. Wang, W. Geng, and H. Xu, *Direct position determination of multiple non-circular sources with a moving coprime array*, IEEE Sens. J. **18** (2018), no. 5, 1–17. https://doi.org/10.1007/s00034-017-0499-4
6. A. F. García-Fernández, M. Morelande, and J. Grajal, *Two-layer particle filter for multiple target detection and tracking*, IEEE Trans. Aerosp. Electron. Syst. **49** (2013), no. 3, 1569–1588. https://doi.org/10.1109/taes.2013.6558005
7. M. Sun, W. Xia, and Y. Wang, *Direct target tracking by distributed Gaussian particle filtering based on delay and Doppler*, (Proc. IEEE Int. Conf. Signal Process., Beijing, China), 2018, pp. 58–63. https://doi.org/10.1109/icsp.2018.8652505
8. A. J. Weiss, *Direct geolocation of wideband emitters based on delay and Doppler*, IEEE Trans. Signal Process. **59** (2011), 2513–2521. https://doi.org/10.1109/tsp.2011.2128311
9. Z. Khan, T. Balch, and F. Dellaert, *MCMC-based particle filtering for tracking a variable number of interacting targets*, IEEE Trans. Pattern Anal. Mach. Intell. **27** (2005), no. 11, 1805–1819. https://doi.org/10.1109/tpami.2005.223
10. Z. Dai, B. Ba, W. Cui, and Y. Sun, *Computational efficient two-dimension DOA estimation for incoherently distributed noncircular sources with automatic pairing*, IEEE Access **5** (2017), 20249–20259. https://doi.org/10.1109/access.2017.2757932
11. T. Zhao, Z. Zhang, H. Chen, L. Qi, and W. Liu, *Augmented quaternion MUSIC method for near-field noncircular sources with a COLD Array*, IEEE Access **8** (2020), 212106–212113. https://doi.org/10.1109/access.2020.3039870
12. Y. Qian, D. Zhao, and H. Zeng, *Direct position determination of noncircular sources with multiple nested arrays: Reduced dimension subspace data fusion*, Wirel. Commun. Mob. Comput. **2021** (2021), 1–10. https://doi.org/10.1155/2021/9950518
13. A. Sidi and A. Weiss, *Delay and Doppler induced direct tracking by particle filter*, IEEE Trans. Aerosp. Electron. Syst. **50** (2014), no. 1, 559–572. https://doi.org/10.1109/taes.2013.120326
14. M. Sun and K. Ho, *An asymptotically efficient estimator for TDOA and FDOA positioning of multiple disjoint sources in the presence of sensor location uncertainties*, IEEE Trans. Signal Process. **59** (2011), no. 7, 3434–3440. https://doi.org/10.1109/tsp.2011.2131135
15. F. Gustafsson, *Particle filter theory and practice with positioning applications*, IEEE Aerosp. Electron. Syst. Mag. **25** (2010), no. 7, 53–81. https://doi.org/10.1109/maes.2010.5546308
16. N. Whiteley, S. Sumeetpal, and S. Godsill, *Auxiliary particle implementation of probability hypothesis density filter*, IEEE Trans. Aerosp. Electron. Syst. **46** (2010), no. 3, 1437–1454. https://doi.org/10.1109/ispa.2007.4383746
17. M. R. Morelande, C. M. Kreucher, and K. Kastella, *A Bayesian approach to multiple target detection and tracking*, IEEE Trans. Signal Process. **55** (2007), 1589–1604. https://doi.org/10.1109/tsp.2006.889470
18. W. Yi, M. R. Morelande, L. Kong, and J. Yang, *A computationally efficient particle filter for multitarget tracking using an independence approximation*, IEEE Trans. Signal Process. **61** (2013), 843–856. https://doi.org/10.1109/tsp.2012.2229999
19. M. Orton and W. Fitzgerald, *A Bayesian approach to tracking multiple targets using sensor arrays and particle filters*, IEEE Trans. Signal Process. **50** (2002), no. 2, 216–223. https://doi.org/10.1109/78.978377
20. Z. Xi and C. Fu, *An improved particle filtering algorithm based on UPF*, Comput. Simul. **2** (2014), no. 31, 336–339.
21. M. Arulampalam, S. Maskell, N. Gordon, and T. Clapp, *A tutorial on particle filters for online nonlinear/non-gaussian Bayesian tracking*, IEEE Trans. Signal Process. **50** (2002), no. 2, 174–188. https://doi.org/10.1109/78.978374
22. C. M. Kreucher, K. Kastella, and A. O. Hero III, *Multitarget tracking using the joint multitarget probability density*, IEEE Trans. Aerosp. Electron. Syst. **41** (2005), no. 4, 1396–1414. https://doi.org/10.1109/taes.2005.1561892
23. C. Guo and J. Luo, *Direct particle tracking algorithm based on MCMC*, J. Hangzhou Dianzi University (Natural Sciences). **41** (2021), no. 2, 48–53.
24. Z. Xi and C. Fu, *Improved particle filter algorithm based on MCMC*, Comput. Eng. Des. **35** (2014), no. 9, 3070–3074.
25. Y. Chen, Y. Wang, F. Qu, and W. Li, *A graph-based track-before-detect algorithm for automotive radar target detection*, IEEE Sens. J. **21** (2021), no. 5, 6587–6599. https://doi.org/10.1109/JSEN.2020.3042079
26. J. M. Pak, C. K. Ahn, Y. S. Shmaliy, and M. T. Lim, *Improving reliability of particle filter-based localization in wireless sensor networks via hybrid particle/FIR filtering*, IEEE Trans Industr Inform **11** (2015), no. 5, 1089–1098. https://doi.org/10.1109/tii.2015.2462771
27. Z. Lu et al., *Direct trajectory determination algorithm based on evolutionary particle filter*, Syst. Eng. And Electron. **40** (2018), no. 5, 968–975.

AUTHOR BIOGRAPHIES

Yang Qian received his M. S degree in Electronic and Communication Engineering from Guangxi University, Nanning, China, in 2019. He is working toward his Ph.D. degree in Communication and Information Systems with the Nanjing University of Aeronautics and Astronautics, Nanjing, China. His research interests include array signal processing, radiation source localization, and tracking.

Xinlei Shi received his B.S. degree in Electronic Information Science and Technology from Jiangsu University of Science and Technology, Zhenjiang, China, in 2021. He is currently working toward his Ph.D. degree in Electronic and Communication Engineering with the Nanjing University of Aeronautics and Astronautics, Nanjing, China. His research interests include signal and information processing and radiation source localization.

Haowei Zeng received his B.S. degree in Information Engineering from Nanjing University of Aeronautics and Astronautics, Nanjing, China, in 2020. He is currently working toward his M.S. degree in Information and Communication Engineering with the Nanjing University of Aeronautics and Astronautics, Nanjing, China. His research interests include direction of arrival, wireless localization, and direct position determination.

Mushtaq Ahmad got his M. S degree in Communication and Information System from Nanjing university of aeronautics and astronautics, Nanjing, China, in 2017, and currently pursuing his Ph. D. degree in the School of Electronics and Communication Engineering, from NUAA, China. His research study interests consist of array signal processing, DOA estimation, and massive MIMO radar system.

How to cite this article: Y. Qian, X. Shi, H. Zeng, and M. Ahmad, *Direct tracking of noncircular sources for multiple arrays via improved unscented particle filter method*, ETRI Journal **45** (2023), 394–403. https://doi.org/10.4218/etrij.2022-0001